Guest–Host Interactions between Crown-Containing 2-Styrylbenzothiazole and HP-*β*-CD

YU.V. FEDOROV[1], O.A. FEDOROVA[1], E.N. ANDRYUKHINA[1], S.P. GROMOV[1], M.V. ALFIMOV[1] and J.J. AARON[2]*

[1]*Photochemistry Center of Russian Academy of Sciences, Novatorov str, 7a, 117421, Moscow, Russia;* [2]*ITODYS, Université Paris 7, CNRS UMR 7086, 1, Rue Guy de la Brosse, 75005 Paris, France*

Abstract

The inclusion complexes of the *trans*-isomer of 2-[2-(6,7,9,10,12,13,15,16-octahydro-5,8,11,14,17-pentaoxa-benzocyclopentadecen-2-yl)-vinyl]-benzothiazole (CSB) with 2-hydroxypropyl-*β*-cyclodextrin (HP-*β*-CD) were investigated by electronic absorption and fluorescence spectroscopies in aqueous solution. The addition of HP-*β*-CD has very little effect on the absorption spectra of CSB. A 17-nm blue shift and pronounced fluorescence enhancements in the emission spectrum of CSB were observed. 1:1 and 1:2 stoichiometries were found for complexes of CSB with HP-*β*-CD, and formation constants of the complexes and other thermodynamic parameters were estimated from fluorescence measurements. In the case of the 1:1 CSB: HP-*β*-CD complex, the formation constant was equal to 3,802 at 293 K, the complexation reaction was exothermic ($\Delta H^0 = -9.2 \pm 1.1$ kJ mol^{-1}) and presented a positive entropy value ($\Delta S^0 = 37.3 \pm 3.8$ J mol^{-1} K^{-1}). A molecular structure was proposed for the CSB:HP-*β*-CD inclusion complex.

Introduction

Condensation of styryl dye molecules with benzocrown ethers results in novel macrocyclic ionophores, which are able to bind metal cations and possess easily recognizable changes in the absorption or fluorescence spectra of the sensor molecule [1–3]. Such compounds are promising for the development of reagents for optical determination of metal cations and as components of photoswitching molecular devices. However, because of their hydrophobicity, crown-containing 2-styrylbenzothiazoles are poorly soluble in aqueous media, which constitutes an important problem for sensitivity of recognition.

It is well known that cyclodextrins (CDs), water-soluble, doughnut-shaped cyclic oligosaccharides consisting of six or more *α*-(1,4)-linked D-glucopyranose units, are able to form inclusion complexes (host–guest complexes) with a wide variety of guest organic molecules possessing suitable polarity and dimension characteristics [4, 5]. Complexation is governed by various types of interactions, including geometrical steric factors, hydrophobic interactions, hydrogen bonding, and London dispersion forces [6]. CDs have received a considerable attention, due to their ability to modify important physical and chemical properties of the included guests. For instance, an increase in the aqueous solubility of lipophilic compounds and an enhancement of the fluorescence emission of some molecules in the presence of CDs have been reported, leading to interesting analytical applications [7–14].

Therefore, the cyclodextrin molecules can be considered as promising components for the building of complexes with crown-containing conjugated heteroaromatic compounds such as 2-styrylbenzothiazole (CSB). Moreover, CSB can bind the alkaline earth metal cations in organic solvents, the complexation being accompanied by changes in fluorescent properties [3]. It can be suggested that the inclusion complexes CD:CSB should be water-soluble and display a more pronounced fluorescent response upon binding with metal cations. The first step of the investigation consists to study the mechanism of formation of the CD:CSB complex, which is the important factor for controlling the supramolecular properties.

In this paper, we report an electronic absorption and fluorescence spectrometric study of the host–guest interactions of HP-*β*-CD with CSB in aqueous media. The stoichiometry and thermodynamic characteristics of the inclusion complexes, including a temperature effect on the complex formation constant, are evaluated and discussed.
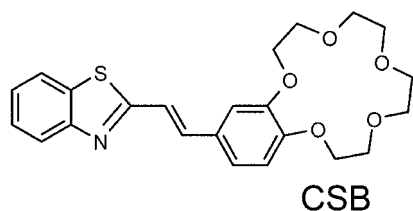
Experimental

Reagents and instrumentation

The synthesis of the *trans*-isomer of 2-[2-(6,7,9,10,12,13,15,16-Octahydro-5,8,11,14,17-pentaoxa-benzocyclopentadecen-2-yl)-vinyl]-benzothiazole (CSB) has been described

---

* Author for correspondence. E-mail: aaron@paris7.jussieu.fr

previously [15]. High-purity HP-β-CD and D-glucose were purchased, respectively, from Aldrich and Merck and were used as received. Ethanol (spectroscopic grade, Merck), acetonitrile (spectroscopic grade, Prolabo) and distilled water were used as solvents.

CSB

Figure 1. 2×10^{-5} M CSB UV-Visible absorption spectra in (a) water-acetonitrile [100:1 v/v (WA)] mixture, (b) ethanol-acetonitrile [100:1 v/v (EA)] mixture, (c) acetonitrile, (d) 10^{-2} M HP-β-CD WA mixture.

Absorption spectra were recorded on a Perkin-Elmer Lambda 2 spectrometer, using 1-cm quartz cuvettes at 20 ± 1 °C. Fluorescence spectra were obtained on a Perkin-Elmer LS-5 luminescence spectrometer equipped with a pulsed xenon lamp and interfaced to a personal computer. The excitation and emission band widths were 5 nm. All fluorescence measurements were carried out in 1-cm quartz cuvettes at different temperatures [10, 20, 30 and 40 ± 0.1 °C], using a cell holder with a thermostatically controlled Bioblock Model 18205 water bath. Fluorescence quantum yields (Φ_F) were measured on a Shimadzu RF-5000 spectrophotofluorimeter.

Procedures

2×10^{-3} M CSB stock solutions were prepared in acetonitrile and kept in the dark to avoid photoisomerization. These solutions were diluted to obtain 2×10^{-5} M CSB working solutions for spectroscopic studies. 10^{-1} M stock solutions of HP-β-CD were prepared in distilled water. The general procedure was to add in the cuvette 25 μl of the CSB stock solution to 2.5 ml of the HP-β-CD initial solution or to 2.5 ml of pure ethanol, acetonitrile or distilled water. Thus, a 2×10^{-5} M concentration of CSB and concentrations of HP-β-CD practically equal to those of the stock solutions were obtained in all cases. For all working aqueous solutions, the water-acetonitrile ratio was 100:1, v/v.

The CSB fluorescence quantum yields were evaluated by means of a 10^{-5} M quinine sulfate solution in 0.5 M H$_2$SO$_4$ as a standard ($\phi_F = 0.55$) [16] and by exciting at 366 nm. Φ_F values were determined by applying the following equation:

$$\Phi_{F,x} = \Phi_{F,r} \frac{(1 - 10^{-A_r})D_x}{(1 - 10^{-A_x})D_r}, \quad (1)$$

where $\Phi_{F,x}$ and $\Phi_{F,r}$ are the fluorescence quantum yields of the analyte and the standard, respectively, A_x and A_r are the absorbances of the analyte and the standard solutions, respectively, and D_x and D_r are the integrated area of the emission fluorescence spectra, corrected for the solvent blank, of the analyte and the standard solutions, respectively.

Quantum mechanical calculations

Quantum mechanical calculations were performed by using HyperChem^{TM}, Release 6.01 for Windows Molecular Modeling System (Hypercube, Inc.). Optimized geometry
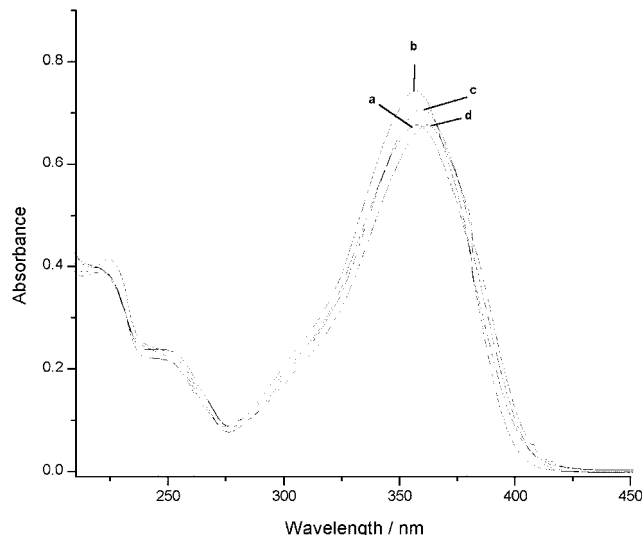
and dipole moment of CSB were calculated by choosing the semi-empirical AM1 method and Polak-Ribiere optimization algorithm.

Results and discussion

Spectral properties

Electronic absorption spectra. UV-Visible absorption spectra of CSB were recorded in aqueous solution of 10^{-2} M HP-β-CD, ethanol, acetonitrile and water (Figure 1, Table 1).

The absorption spectrum of CSB in water-acetonitrile [100:1 v/v (WA)] mixture is characterized by an intense long-wavelength band with a maximum absorption at 358 nm and two shoulders or secondary peaks in the 220–225 nm and 245–255 nm regions. The long-wavelength absorption band maxima and the corresponding molar absorption coefficients values do not change significantly in ethanol, acetonitrile and HP-β-CD media. It was found that the CSB spectrum in HP-β-CD shows only a 4-nm red-shift of the long-wavelength absorption band, upon going from water (358 nm) to HP-β-CD (362 nm). Weak increase of molar absorption coefficient are observed in acetonitrile and ethanol relative to water and HP-β-CD medium.

Fluorescence spectra. Fluorescence emission and excitation spectra of CSB recorded in ethanol, acetonitrile, and in water in the absence and the presence of HP-β-CD are shown in Figures 2 and 3.

The excitation spectra are characterized by poorly-resolved bands located at 245–250 nm, 340–345 nm and 375–383 nm. These spectral features are similar in the various media under study. The emission spectra exhibit a broad, structureless band, located at 460.5 nm in WA, 435.5 nm in EA, 439 nm in acetonitrile and 443.5 nm in the HP-β-CD medium. The shapes of the emission spectra are essentially

Table 1. Electronic absorption and fluorescence spectral characteristics of CSB[a] in the different media under study

Medium	Absorption λ/nm (ϵ_{max}/10^4 M^{-1} cm^{-1})	Fluorescence		Stokes shift[b]/cm^{-1}	ϕ_F[c]
		λ_{ex}/nm	λ_{em}/nm		
Water	358 (3.4)	381sh[e]	460.5	6217	0.0053
	250 sh[e]	343			
	222 sh[e]	246			
MeCN	357 (3.7)	375.5	439	5232	0.0069
	250sh[e]	341.5			
	224 (2.1)	248			
EtOH	359 (3.5)	380.5	435.5	4893	0.0059
	250 sh[e]	339.5			
	221 (1.9)	248			
HP-β-CD (0.1 M)[d]	362 (3.4)	383	443.5	5076	0.027
	246 (1.2)	340.5			
	222 sh[e]	248 sh[e]			

[a]CSB concentration is 2×10^{-5} M.
[b]Stokes shift: $\nu_{max}^{abs} - \nu_{max}^{em}$.
[c]Quantum yields measured at $\lambda_{ex} = 366$ nm relative to a 0.5 M H$_2$SO$_4$ quinine sulfate aqueous solution ($\phi_f = 0.55$).
[d]Solvent: water-acetonitrile (100:1 v/v).
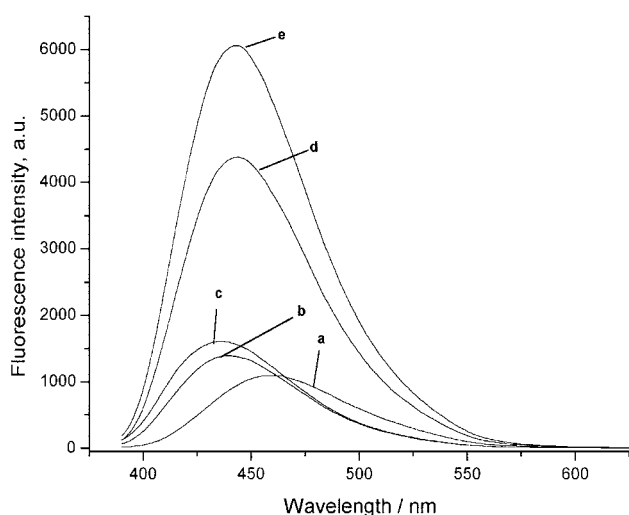[e]sh means shoulder.

Figure 2. Fluorescence emission spectra of 2×10^{-5} M CSB in (a) water-acetonitrile [100:1 v/v (WA)] mixture, (b) ethanol-acetonitrile [100:1 v/v (EA)] mixture, (c) acetonitrile, (d) 10^{-2} M HP-β-CD WA mixture, (e) 10^{-1} M HP-β-CD WA mixture at 293 K.

Figure 3. Fluorescence excitation spectra of 2×10^{-5} M CSB in (a) water-acetonitrile [100:1 v/v (WA)] mixture, (b) ethanol-acetonitrile [100:1 v/v (EA)] mixture, (c) acetonitrile, (d) 10^{-1} M HP-β-CD WA mixture.

similar in all media under study. As can be seen, a 17-nm blue-shift is observed in HP-β-CD relative to water.

The fluorescence quantum yields of CSB present very close values, ranging between 0.0053 and 0.0069 in water, ethanol and acetonitrile, whereas a 5-fold increase of Φ_F is observed in 0.1 M HP-β-CD relative to water (Table 1).

These observations are in agreement with the formation of an inclusion complex between CSB and the HP-β-CD, which would increase the CSB first excited singlet state energy level and diminish the radiationless deactivation process rates.
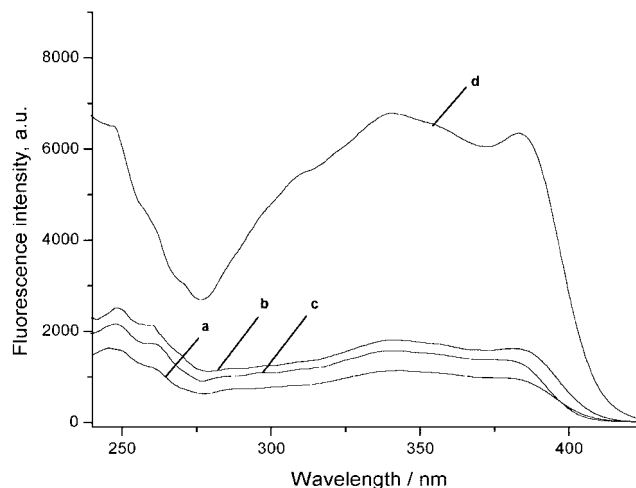
Effect of cyclodextrin concentration

We investigated the effect of the addition of HP-β-CD on CSB UV-visible absorption and fluorescence spectra in the range 0–10^{-1} M. As already mentioned, the addition of HP-β-CD produces only a small 4-nm red-shift in the absorption spectrum of CSB and no molar extinction coefficient significant change was observed at the absorption maximum (Table 1).

The effect of increasing the HP-β-CD concentration on the fluorescence spectrum of CSB was studied by exciting at the lowest energy absorption band. The fluorescence intensities of CSB were enhanced progressively upon adding HP-β-CD, and a shift of the emission maximum occurred from 460 to 443 nm (Figure 4 and Table 1).

When plotting the CSB fluorescence intensity *vs.* HP-β-CD concentration, a levelling-off curve was obtained (Figure
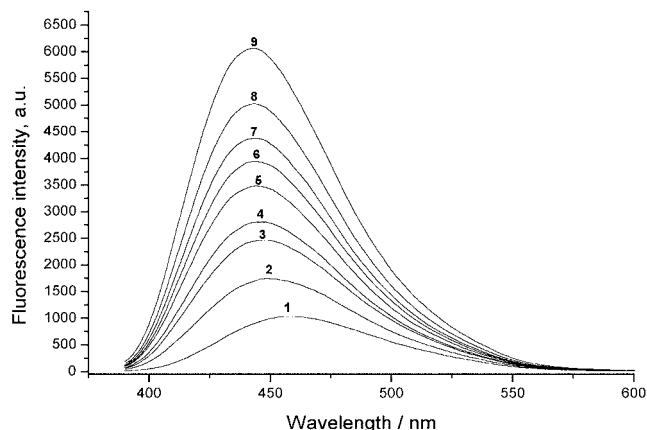
Figure 4. Variation of the 2×10^{-5} M CSB fluorescence emission spectra with increasing [HP-β-CD] at 293 K: (1) 0, (2) 1, (3) 2, (4) 4, (5) 10, (6) 20, (7) 100, (8) 400, (9) 1000 $\times 10^{-4}$ M.
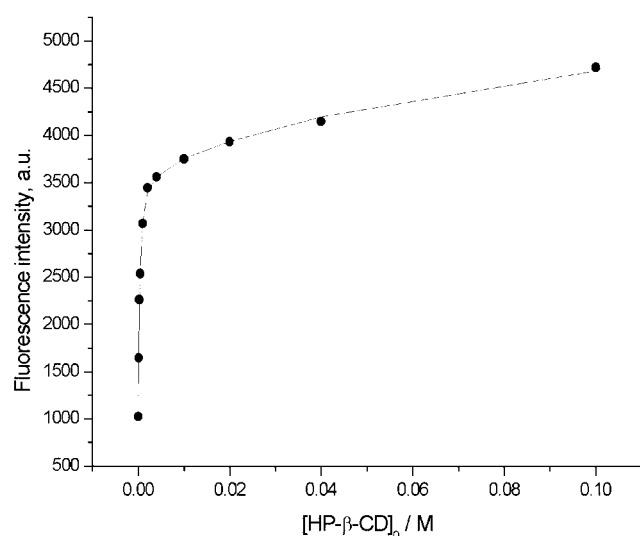

Figure 5. Influence of HP-β-CD concentration on the fluorescence intensity (at λ_{em} = 450 nm) of a 2×10^{-5} M CSB WA solution at 293 K. The solid line was calculated by applying Hyperquad program, assuming a 1:1 and 1:2 stoichiometries (CSB : HP-β-CD) and stability constants log K_1 = 3.58 and log K_2 = 4.7.

5). The enhancement of the fluorescence intensity by HP-β-CD was rapid in the range 0.0001–0.004 M HP-β-CD. Further increase of HP-β-CD concentration towards 0.1 M did not lead to the usual plateau region. Instead, it was observed an additional slow increase of the fluorescence intensity resulting probably from formation of more than one host:guest complex.

To find out whether the spectral changes observed could be due only to a solvent effect related to the HP-β-CD high concentration, the influence of D-glucose was tested. As with HP-β-CD, D-glucose (0.7 M) enhanced the fluorescence intensity of CSB. However, the effect of glucose on the CSB fluorescence spectrum and intensity is negligible as compared to that produced by HP-β-CD. Indeed, the emission maximum was red shifted by only 3 nm and a 7% fluorescence intensity increase was observed in the presence of 0.7 M D-glucose (Figure 6). Therefore, this result confirms the formation of inclusion complexes between CSB and HP-β-CD.
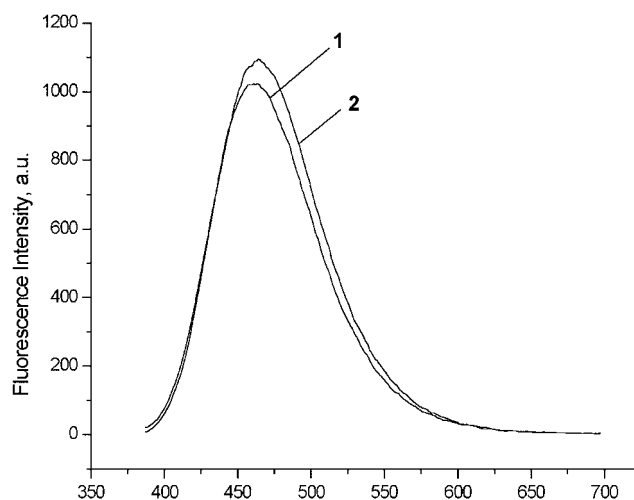

Figure 6. Fluorescence emission spectra of 2×10^{-5} M CSB in water-acetonitrile [100:1 v/v (WA)] mixture (1) and 0.7 M D-glucose WA mixture (2) at 293 K.

Stoichiometry and association constants of the inclusion complexes

The enhancement of the fluorescence of CSB upon HP-β-CD concentration increasing allows to define the stoichiometry of the CSB-HP-β-CD inclusion complexes and to determine their association constants.

A Benesi–Hildebrand linear regression analysis was used to obtain information on the stoichiometry of the complexes. The relation between the increase of the CSB fluorescence intensity and the HP-β-CD concentration can be represented by the following equation in the case of a 1:1 stoichiometry [17]:

$$\frac{1}{F - F_0} = \frac{1}{F_\infty - F_0} + \frac{1}{(F_\infty - F_0) \cdot K_1 \cdot [\text{HP} - \beta\text{CD}]_0}. \quad (2)$$

If the stoichiometry of the complex is assumed to be 1:2, Equation (2) becomes applicable:

$$\frac{1}{F - F_0} = \frac{1}{F_\infty - F_0} + \frac{1}{(F_\infty - F_0) \cdot K_2 \cdot [\text{HP} - \beta\text{CD}]_0^2}. \quad (3)$$

In Equations (2) and (3), F_0 and F_∞ denote, respectively, the fluorescence intensity of CSB in the absence of HP-β-CD and when all CSB molecules are essentially complexed with HP-β-CD. F is the measured fluorescence at each CD concentration tested. [HP-β-CD]$_0$ is the initial HP-β-CD concentration, K_1 and K_2 are, respectively, the association constants of the complex with 1:1 and 1:2 stoichiometries. If the stoichiometry is 1:1, a linear plot of $1/(F - F_0)$ *vs.* $1/$[HP-β-CD]$_0$ should be obtained. In the case that the 1:2 stoichiometry is predominant, a plot of $1/(F - F_0)$ *vs.* $1/$[HP-β-CD]$_0^2$ should give a straight line.

Double reciprocal plots obtained from fluorescence data when Equations (2) and (3) were applied are shown in Figures 7 and 8.
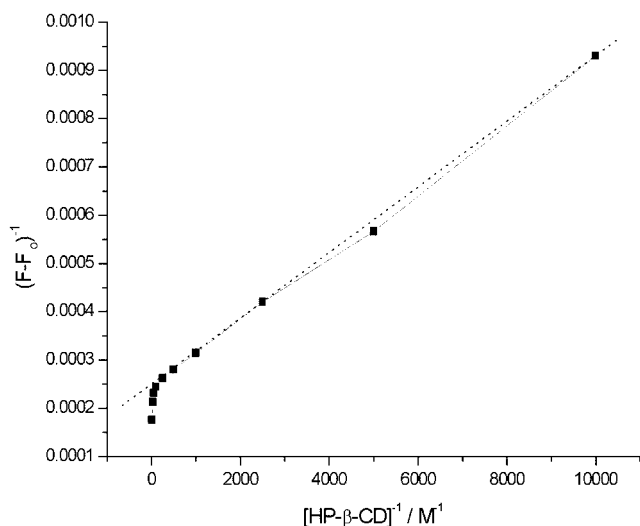
Figure 7. Benesi–Hildebrand plot for CSB complexed to HP-β-CD at 20 °C assuming 1:1 CSB: HP-β-CD stoichiometry.
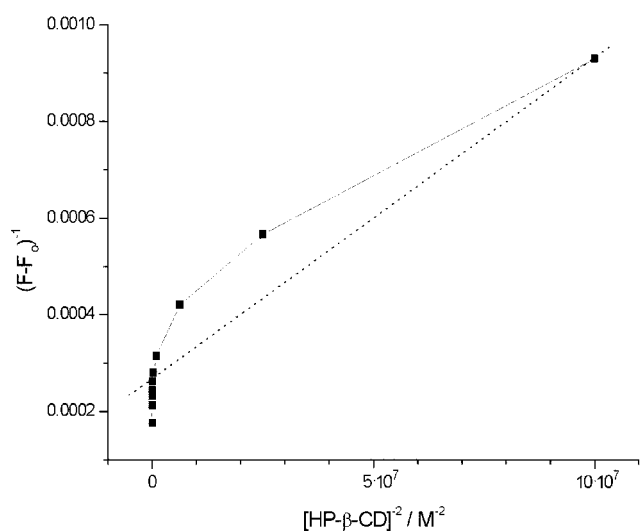

Figure 8. Benesi-Hildebrand plot for CSB complexed to HP-β-CD at 20 °C assuming 1:2 CSB: HP-β-CD stoichiometry.

A typical linear double-reciprocal plot was established only in the concentration range 0.0001–0.004 M for HP-β-CD when applying Equation (2), which indicates a 1:1 stoichiometry for the inclusion complex of CSB with HP-β-CD (Figure 7). In contrast, a downward curve was observed, when these data were fitted to a 1:2 complex, using Equation (3) (Figure 8). This curved plot means that simultaneous formation of a 1:2 complex does not take place. However, the sequential formation of 1:1 plus 1:2 complexes, with both complexes occurring at the equilibrium, could also give a nonlinear plot. The double-reciprocal plot curvature found for HP-β-CD concentrations higher than 0.004 M when Equation (2) was applied (Figure 7), also supports the possibility of a sequential formation of 1:1 plus 1:2 complexes at high HP-β-CD concentration. The hypothesis of more than one CSB-HP-β-CD complex formation seems reasonable when considering the respective sizes and structures of the CSB molecule and the HP-β-CD cavity. Indeed, the internal diameter of the HP-β-CD cavity is approximately 7 Å and
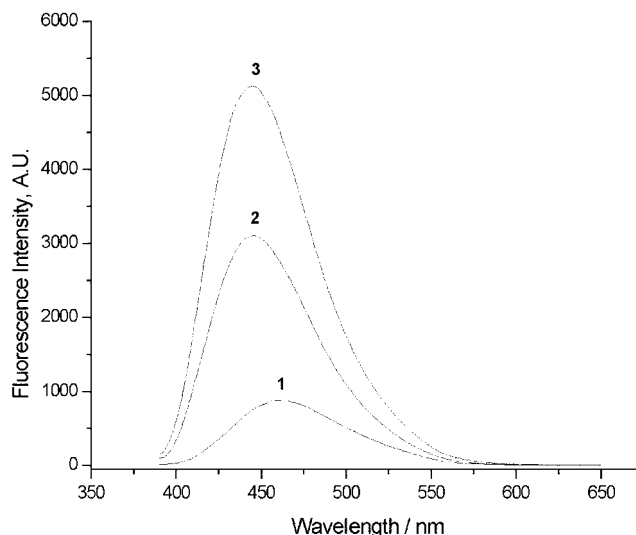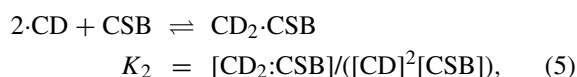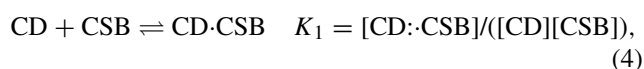

Figure 9. Fluorescence emission spectra of CSB (1) and its complexes CSB:HP-β-CD (2), CSB:(HP-β-CD)$_2$ (3) at 30 °C calculated from the spectrofluorometric titration data by HYDRASP program.

its height is 8 Å. According to semi-empirical calculations based on the quantum mechanical molecular AM1 method [18], the CSB molecule is approximately 19 Å long and 5 to 8 Å wide. Therefore, since only one half of a molecule of CSB can fit the HP-β-CD cavity, simple geometrical considerations would support the formation of two kinds of CSB-HP-β-CD complexes with 1:1 and 1:2 stoichiometries correspondingly.

To evaluate the association constants of the inclusion complexes calculated from the fluorimetric data, the computer program HYPERQUAD [19] was used. This program is based on a least-squares approach, allowing to obtain best fit equilibrium constant values from potentiometric and/or spectrophotometric data. In HYPERQUAD program, we used normalized spectrofluorimetric titration data instead of spectrophotometric data. The fluorescence emission intensity data at about 10 different wavelengths in the range 440–500 nm were analyzed and the association constants of the complexes formed according to Equations (4) and (5) were determined (Table 2).

$$CD + CSB \rightleftharpoons CD \cdot CSB \quad K_1 = [CD \cdot CSB]/([CD][CSB]), \quad (4)$$

$$2 \cdot CD + CSB \rightleftharpoons CD_2 \cdot CSB$$
$$K_2 = [CD_2 : CSB]/([CD]^2[CSB]), \quad (5)$$

The fluorescence emission spectra of complexes were calculated using the determined equilibrium constant values and the HYDRASP program, included in the HYPERQUAD suite of programs (Figure 9).

Temperature effects

We studied the temperature effect on the CSB: HP-β-CD inclusion complex fluorescence spectra and the thermodynamic characteristics in the 10–40 °C range. No significant

Table 2. Temperature effect on K for the complexation reaction of CSB and HP-β-CD

$T/°C$	Log K_1	Log K_2
10	3.637 ± 0.01	4.8 ± 0.15
20	3.578 ± 0.01	4.7 ± 0.15
30	3.546 ± 0.01	4.7 ± 0.15
40	3.467 ± 0.01	4.8 ± 0.15

Table 3. Selected geometrical dimensions of CSB[a]

Interatomic distance[b]/Å		Torsion angle[b]/°	
H8···H51	18.7946	C5-N55-C11-C32	179.3
H8···O19	13.7355	C4-S54-C11-C32	−179.4
H8···O18	12.9449	N55-C11-C32-C31	0.935
H9···H10	5.0424	C11-C32-C31-C12	−178.2
H34···H35	5.0109	C12-C17-C16-O18	173.4
H37···H41	6.0516	C17-C16-O18-C20	74.9
H38···H42	8.5049	C14-C15-O19-C23	67.9

[a]Calculated by the AM1 method.
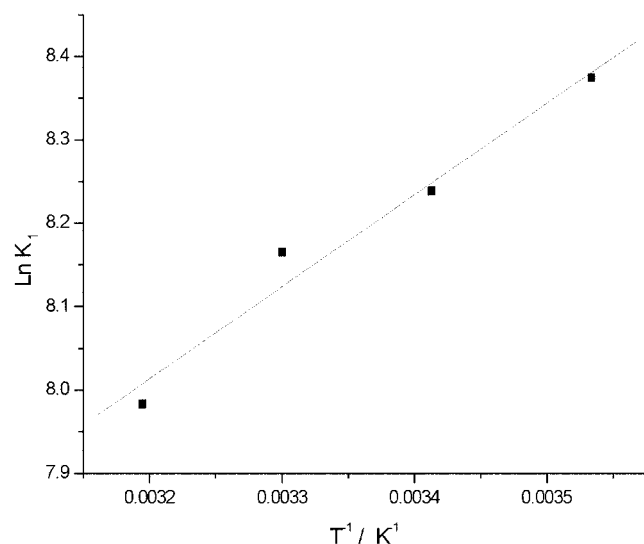[b]Atom numbering corresponds to that given in Figure 11.

Figure 10. Vant' Hoff plot of ln K_1 vs. 1/T for the CSB: HP-β-CD inclusion complex.

change was found in the structure and position of the emission fluorescence spectra upon varying the temperature, whereas a moderate decreasing of fluorescence intensity was observed upon increasing the temperature. This latter effect suggests that the formation of the inclusion complex is not favored at higher temperatures. Indeed, the inclusion complex formation constant values diminished from log K_1 = 3.64 to log K_1 = 3.47 between 10 and 40 °C (Table 2).

To evaluate the thermodynamic parameters of the complexes, we plotted ln K_1 vs. 1/T. A linear relationship (r = 0.985) was established (Figure 10), indicating that the Van t' Hoff equation was obeyed.

The value of the formation enthalpy (ΔH^0) obtained for the complex of CSB with HP-β-CD was -9.2 ± 1.1 kJ mol^{-1}, which shows that the complexation process is exothermic. The positive value of the formation entropy ($\Delta S^0 = 37.3 \pm 3.8$ J mol^{-1} K^{-1}) means that an increase of the disorder occurs during the complexation reaction, which might result from the contribution of water molecules to the process [14]. Indeed, it can be expected that the inclusion process is characterized by a release of water molecules, originally solvated to both the HP-β-CD and the CSB molecules, into bulk water. The Gibbs energy value at 298 K is negative ($\Delta G° = -20.0$ kJ mol^{-1}), indicating that the formation of the inclusion complex is energetically favorable.

Proposed molecular structure of the CSB:HP-β-CD inclusion complexes

We propose a molecular structure for the CSB:HP-β-CD inclusion complexes, based on AM1 method semiempirical calculations and geometrical considerations relative to the size of both species. The HP-β-CD cavity dimensions are similar to those of β-CD (length 7.9 Å and internal diameter 7.8 Å) [5]. The Hyperchem program was used to optimize the CSB molecular structure (Figure 11). The selected interatomic distances and torsion angles of CSB are given in Table 3.

Because of its length [$r(H_8–H_{51})$ = 18.79 Å], CSB can be included only axially in HP-β-CD. The interatomic distances [$r(H_{34}–H_{35})$ = 5.01 Å, $r(H_9–H_{10})$ = 5.04 Å] corresponding to the width of uncrowned moiety of CSB, would clearly be in favor of the inclusion of this moiety in the HP-β-CD cavity. On the other hand, the width of the crown ether moiety [$r(H_{38}–H_{42})$ = 8.5 Å] is larger than the internal diameter of the HP-β-CD cavity and the inclusion of this moiety should be impossible or, taking into account the high flexibility of crown ether, at least more difficult, due to the steric hindrance interactions. Since the longitudinal dimension of CSB is larger than the cavity length of HP-β-CD, CSB would be only partially included in the HP-β-CD cavity, forming a 1:1 CSB:HP-β-CD complex. Furthermore, when taking into account the calculated geometrical dimensions of CSB, there exists a possibility for a second molecule of HP-β-CD to interact with the CSB:HP-β-CD inclusion complex; therefore, the formation of a CSB:(HP-β-CD)^2 inclusion complex could be expected.

We also computed the ground state dipole moment (μg) of CSB, which is equal to 3.86 D. In the inclusion complex, the CSB dipole should take a nearly antiparallel orientation relative to the HP-β-CD dipole, in order to maximize the dipole–dipole interactions. A simplified molecular structure of the expected CSB:HP-β-CD and CSB:(HP-β-CD)$_2$ inclusion complexes are presented in Figure 12. The formation of additional hydrogen bonds between oxygen atoms of the CSB crown ether moiety and hydroxypropyl substituents of HP-β-CD molecules could be expected for the CSB:HP-β-CD inclusion complex, as shown in Figure 12, and this interaction could be an important factor of stability of inclusion complex. Actually, the CSB inclusion complex first formation constant value is very high (K_1 = 3800 M^{-1}) as
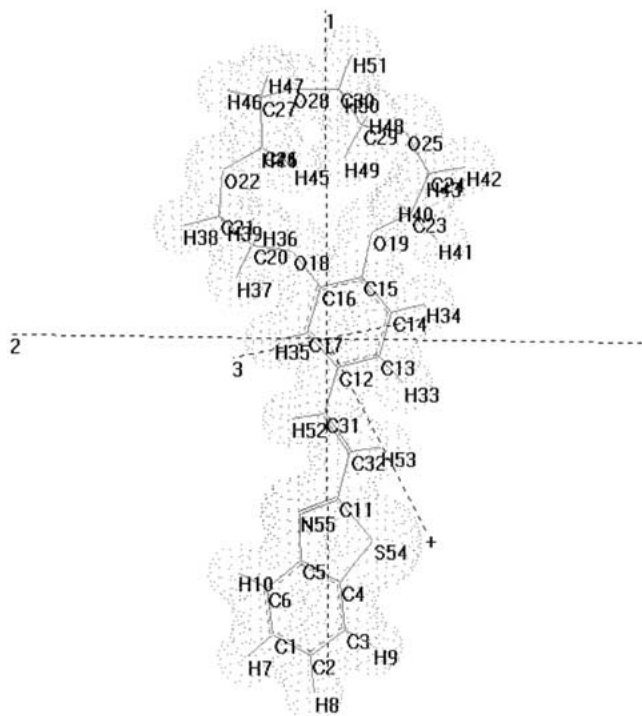
Figure 11. Calculated molecular structure of CSB (μg = 3.85789 D {3.34769; 0.933491; 1.67479}).
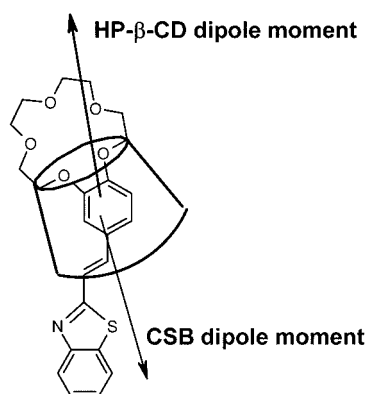

Figure 12. Schematic structures of the CSB : HP-β-CD and CSB : (HP-β-CD)$_2$ inclusion complexes.

compared to cyclodextrin complex formation constant values of other heteroaromatic molecules such as unsubstituted benzophenothiazine [20].

Conclusion

On the basis of the electronic absorption and steady-state fluorescence spectral measurements, the interactions between CSB and HP-β-CD in aqueous solutions were investigated. The significant increase of the fluorescence intensity value with HP-β-CD concentration clearly demonstrates the formation of inclusion complexes between CSB and HP-β-CD. The fluorescence quantum yield of CSB is enhanced by 5 times in HP-β-CD relative to water. Using the

Benesi–Hildebrand method, we found a 1:1 stoichiometry for the inclusion complex at concentrations of HP-β-CD ranging from 0 to 0.004 M. At higher HP-β-CD concentrations the sequential formation of 1:1 and 2:1 host:guest complexes very probably takes place. The association constants for the inclusion complexes were evaluated using HYPERQUAD program. The values of association constant for the 1:1 inclusion complex go from log K_1 = 3.64 to log K_1 = 3.47 in the 10–40 °C temperature range. As shown by the positive entropy value obtained for complexation, the inclusion process is characterized by a release of water molecules originally solvated to both the HP-β-CD and the CSB molecules into the bulk water. AM1 calculations allow us to conclude that the insertion of CSB in the HP-β-CD cavity takes place very probably along the molecular axis with a nearly anti-parallel dipole-dipole orientation.

Acknowledgements

References

1. M.V. Alfimov and S. P. Gromov: in W. Rettig, B. Strehmel, S. Schrader, and H. Seifert (eds.), *Applied Fluorescence in Chemistry, Biology, and Medicine.* Springer-Verlag (1999), pp. 161–178.
2. O.A. Fedorova, Y.V. Fedorov, A.I. Vedernikov, S.P. Gromov, O.V. Yescheulova, M.V. Alfimov, M. Woerner, S. Bossmann, A. Braun, and J. Saltiel: *J. Phys. Chem. A* **106**, 6213 (2002).
3. Y.V. Fedorov, O.A. Fedorova, S.P. Gromov , M. B.Bobrovskii, E.N. Andryukhina, and M.V. Alfimov: *Russ. Chem. Bull.* **51**, 789 (Engl. Transl.) (2002).
4. M.V. Rekharsky and Y. Inoue: *Chem. Rev.* **98**, 1875 (1998).
5. L. Szejtli: *Cyclodextrin Technology*, Kluwer Academic, 1988.
6. K.H. Frömming and J. Szejtli: in J.E.D. Davies (ed.), *Topics in Inclusion Science: Cyclodextrins in Pharmacy*, Kluwer Academic Publishers, 1994.
7. I. Durán-Merás, A. Muñoz de la Peña, F. Salinas, and I. Rodríguez Cáceres: *Analyst* **119**, 1215 (1994).
8. M. Maafi, C. Lion, and J.J. Aaron: *J. Incl. Phenom. Mol. Recogn. Chem.* **30**, 227 (1998).
9. A. Coly and J.J. Aaron: *Anal. Chim. Acta* **360**, 129, (1998).
10. M. Maafi, M.C. Mahedero, and J.J. Aaron: *Talanta* **44**, 2193 (1997).
11. J. Velasco, P. Guardado, C. Carmona, M. A. Muñoz, and M. Balón: *J. Chem. Soc., Faraday Trans.* **94**, 1469 (1998).
12. G.M. Escandar: *Analyst* **124**, 587 (1999).
13. J.A. Arancibia and G.M. Escandar: *Analyst* **124**, 1833 (1999).
14. M.D. Gaye Seye, C. Prot, A. Adenier, J.J. Aaron, and N. Motohashi: *New J. Chem.* **25**, 1290 (2001).
15. Yu.V. Fedorov, O.A. Fedorova, E.N. Andryukhina, S.P. Gromov, M.V. Alfimov, L.G. Kuzmina, A.V. Churakov, J.A.K. Howard, and J.J. Aaron: *New J. Chem.* **27**, 280 (2003).
16. J.N. Demas and G.A. Crosby: *J. Phys. Chem.* **75**, 991 (1971).
17. K.A. Connors: *Binding Constants: The Measurements of Molecular Complex Stability*, John Wiley and Sons, 1987.
18. M.J.S. Dewar, E.G. Zoebisch, and E.F. Healy: *J. Amer. Chem. Soc.* **107**, 3902 (1985).
19. P. Gans, A. Sabatini, and A. Vacca: *Talanta* **43**, 1739 (1996).
20. M. Maafi, J.J. Aaron, M.C. Mahedero, and F. Salinas: *Appl. Spectrosc.* **52**, 91 (1998).